Detection and tracking of airplanes on runways with passive radar data

Martina Broetje
Dept. Sensor Data and Information Fusion
Fraunhofer FKIE
D-53343 Wachtberg, Germany
Email: martina.broetje@fkie.fraunhofer.de

***Abstract*—This paper discusses the use of a passive radar experimental system based on mobile communication signals for detecting and tracking airplanes on the airport runways. We employ a two-stage strategy, taking advantage of the fact that the estimation region is limited to the runways. In the first stage, we focus the detection of moving targets in the passive radar data. In the second stage, we classify the runway targets and determine their location on the runway. This also involves a classification task, where the detections are assigned to specific runways or other moving objects such as flying airplanes. The approach is evaluated with data from a measurement campaign conducted at Frankfurt airport.**

I. Introduction

In the airport area, various sensors are used to enhance air traffic safety. The commonly used surveillance methods include active radar and camera (EO/IR) sensors. Also multilateration systems are in use for wide area and airport surveillance [1]. Other possible sensors could be LIDAR sensors [2], sensors detecting seismic vibration [3] and direction finding sensors [4]. Each sensor has its own advantages and weaknesses. EO/IR and LIDAR sensors are capable of detecting small objects, but they require a dense network of sensors due to their limited range. Multilateration systems offer good localization capabilities and are suitable for wide area surveillance. However, these systems rely on signals transmitted by the target, which can, e.g., result in limited update rates due to varying transmission times. Also, direction finding sensors have a good range, but require that the target sends a radio frequency signal. They provide accurate direction information but no range information. Radar systems, including passive radar, can detect silent targets. Passive radar systems utilize existing broadcast transmitters instead of installing separate transmitters and have several advantages and challenges [5]–[7], such as achieving high update rates. They benefit from multistatic configurations, where multiple transmitters can be evaluated with a single receiver.

In the last decades, passive radar has emerged as a proven technology for detecting and tracking targets in airspace, as demonstrated, e.g., in [8]. When focusing on the airspace, traffic from ground is usually filtered. The Fraunhofer FKIE has developed experimental passive radar systems that utilize mobile communication signals. Here, we focus on illumination using Global System for Mobile (GSM) communications signals. While GSM is not suitable for wide area surveillance due to its low transmit power, it offers the advantage of a high availability of transmitters and relatively high frequency, resulting in a good discrimination of targets in terms of range-rate and the ability to detect small targets. Therefore, the focus lies on maritime harbor protection and drone detection scenarios. A discussion of feasibility is provided in [9], [10]. In the current work GSM passive radar is applied to monitor the runway for rolling airplanes. The low altitude and nearby targets are suitable for illuminators with low power. A passive radar tracking approach usually utilizes the detection of the same target from multiple transmitters, thus benefits from geometrical diversity for detection and localization. We discussed a multi-stage association architecture in [11], [12] which is able to track targets in three dimension. In this paper, we restrict the target state space to the runways and analyze the capability of target detection and tracking. We have developed a two-stage scheme for our research. In the first stage, we focus on detecting moving targets using Range/Doppler tracking in measurement coordinates for a single receiver and transmitter pair. In a next stage, we generate Cartesian estimates by applying non-linear regression, with the constraint that the target is located on the runway. The main objective is to determine whether the target is on the runway and, if so, which specific runway it is on. Inspired by the approach in [13], the test relies on thresholding based on a distance measure. Specifically, we use the Mahalanobis-distance in measurement coordinates.

In the next section we provide details about the measurement setup during the campaign at Frankfurt airport. We then describe the tracking method developed for application to the airport passive radar scenario in Section IV. Finally, results will be discussed in Section V.

II. Passive radar measurement model

A bistatic radar system consists of a transmitter (Tx) and receiver (Rx), which are spatially separated with Tx located at $\boldsymbol{s} = (s_x, s_y, s_z)$ and Rx located at $\boldsymbol{o} = (o_x, o_y, o_z)$. A signal is emitted by the Tx and is reflected at the target at $\boldsymbol{q} = (x, y, z)$ (see Fig. 1(a)) producing an echo of the original signal. Comparing the emitted signal with the received target echo the target state parameters can be estimated. Since the

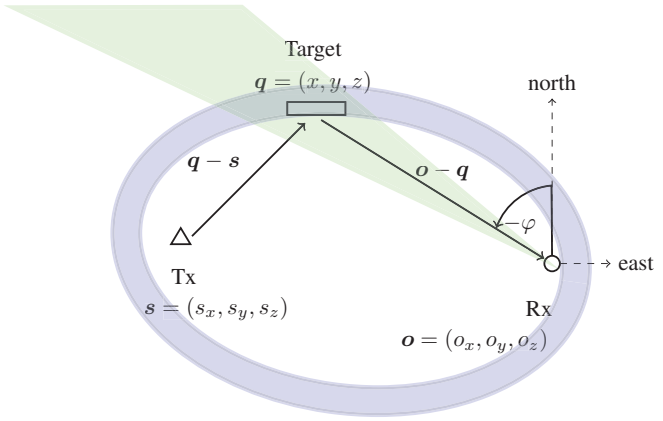

Fig. 1. Bistatic Setup; signal from transmitter at $\boldsymbol{s}$ is reflected by the target at $\boldsymbol{q}$ and received at the observer $\boldsymbol{o}$.

time of transmission is usually unknown, the Time Difference of Arrival (TDoA) τ between the time of arrival of the direct signal, i.e. the Tx signal propagating on a direct path between Tx and Rx, and the time of arrival of the reflected signal is measured. From the known distance between the transmitter and receiver $||\boldsymbol{o} - \boldsymbol{s}||$ the bistatic range is calculated by $r = \tau \cdot c + ||\boldsymbol{o} - \boldsymbol{s}||$.

The contours of constant bistatic range describe ellipses in 2D Cartesian and ellipsoids in 3D Cartesian coordinates. In dependency on the Cartesian position of the target $\boldsymbol{q}$ the bistatic range equation is given by

$$r = ||\boldsymbol{q} - \boldsymbol{o}|| + ||\boldsymbol{q} - \boldsymbol{s}||. \tag{1}$$

To describe the Doppler shift f_d as a function of the target state we use the bistatic range-rate $\dot{r}$ given by

$$\dot{r} = -f_d \lambda = \left(\frac{\boldsymbol{q} - \boldsymbol{o}}{||\boldsymbol{q} - \boldsymbol{o}||} + \frac{\boldsymbol{q} - \boldsymbol{s}}{||\boldsymbol{q} - \boldsymbol{s}||} \right)^T \cdot \boldsymbol{v} \tag{2}$$

where $\boldsymbol{v} = (\dot{x}, \dot{y}, \dot{z})$ is the velocity vector of the target. Transmitter and receiver are assumed stationary.

The direction of arrival (DoA) of the echo signal can be determined using an array antenna. We consider here the DoA in the x-y plane (azimuth). It is related to the geometry by the four-quadrant inverse tangent

$$\varphi = \text{atan2}\Big(x - o_x, y - o_y\Big) \in (-\pi, \pi] \tag{3}$$

When defining the target state vector by $\boldsymbol{x} = (\boldsymbol{q}, \boldsymbol{v}) = (x, y, z, \dot{x}, \dot{y}, \dot{z})$ the functional relationship between target state and measurements for the i-th transmitter and receiver pair can be expressed by the non-linear measurement equation $\mathbf{h}^{(i)}(\boldsymbol{x}) = (h_r^{(i)}, h_{\dot{r}}^{(i)}, h_\varphi^{(i)}) = (r, \dot{r}, \varphi)$, which is defined by equations (1), (2) and (3).

The performance of the passive radar system is described by the characteristic values of the signal and the receiving antenna. For GSM the effective band width is about 81 kHz, the transmit power is about 10 W and the frequency is about 900 or 1800 MHz. This values define the detection range and the measurements resolution, which are additionally influenced by the system parameters integration time and antenna aperture size [14]–[16]. GSM passive radar delivers relative low detection ranges and poor range resolution (about 1800 m) which need to be considered in the system and tracking design. The resolution in range-rate is quite good, due to the relatively high signal frequency. Note that the measurements accuracy is usually better than the measurements resolution.

Fig. 2. GSM passive radar antenna

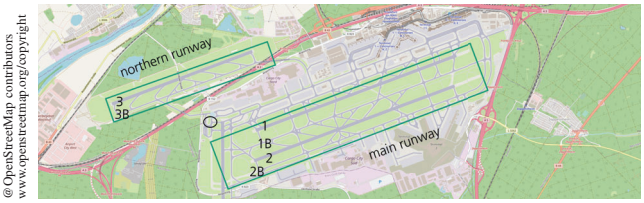

Fig. 3. Measurement campaign at Frankfurt Airport. The receiver was positioned at the black circle. This placement allowed focusing on either the main runways or the northern runway. The numbering of the runways is arbitrary and does not reflect any true occupancy.

III. Measurement Campaign

A measurement campaign with the Fraunhofer FKIE GSM passive radar experimental system has been conducted at Frankfurt airport in Germany. The receiver antenna was placed at a tower (see Fig. 2), allowing for adaptation of the antenna heading to focus on different regions of the airport area, see Fig. 3. Due to the presence of numerous potential transmitters near the airport, a mission planning tool [17] was utilized to limit the number of transmitters in preparation of the campaign. The experimental system can currently process up to five transmitters simultaneously. Thus, during the campaign different configurations of transmitters were tested, and long-term measurements were conducted with the preferred setups to analyze different airplane types and trajectories.

Reference trajectories (so called groundtruth, GT) was provided by Fraport AG from ADS-B and Multilateration sensors. By using the ICAO number, the type or size of the airplane could be identified.

IV. METHOD

Our conventional tracking and fusion strategy for passive radar systems is based on the algorithm described in [11]. It consists of three partially interacting tracking stages:

- The first stage (Range/Doppler tracking) performs MHT tracking in measurement coordinates individually for each Tx/Rx pair.
- The second tracking stage (correlation stage) addresses the multi-sensor association step. Different association possibilities are tested and the "best" (according to a scoring function) multi-target interpretation of all Range/Doppler tracks is provided as output. In this stage the measurment information is transformed into Cartesian coordinates generating Cartesian tracks.
- The third stage (Cartesian tracking) is performed only for tracks with high score. These are tracks from the second tracking stage with high probability of belonging to a true target. Here we apply a standard centralized version of the MHT.

We found multi-stage tracking to provide a good compromise between robustness and precision [11].

Therefore, we use this approach as a basis for the detection and localization of aircrafts on the runways, adressing the following tasks:

A. Detect moving targets in measurement coordinates
B. Localize and classify targets on the runway

A. Detect moving targets in measurement coordinates

Analogue to [11] we use a Multihypothesis tracking (MHT) approach in measurement coordinates for each individual Tx/Rx pair. The state vector is defined by $(r, \dot{r}, \ddot{r}, \varphi, \dot{\varphi})$. We utilize a nearly constant acceleration model for the range/range-rate component and a nearly constant velocity model for the azimuth component. The MHT employs a sequential Likelihood Ratio test for track extraction. The result is a Range/Doppler (R/D) track, which consists of a collection of measurements over time that have been validated to belong to the same moving target rather than originating from false alarms.

In Fig. 4 measurements of a single Tx/Rx pair are shown in the Doppler versus time display. In Fig. 4 below the identified tracks are displayed in white color. For this Tx/Rx geometry we identify the contributions of landing airplanes in the positive Doppler area and of starting airplanes in the negative Doppler area. Note, that there is a region of increased Clutter near to Doppler zero.

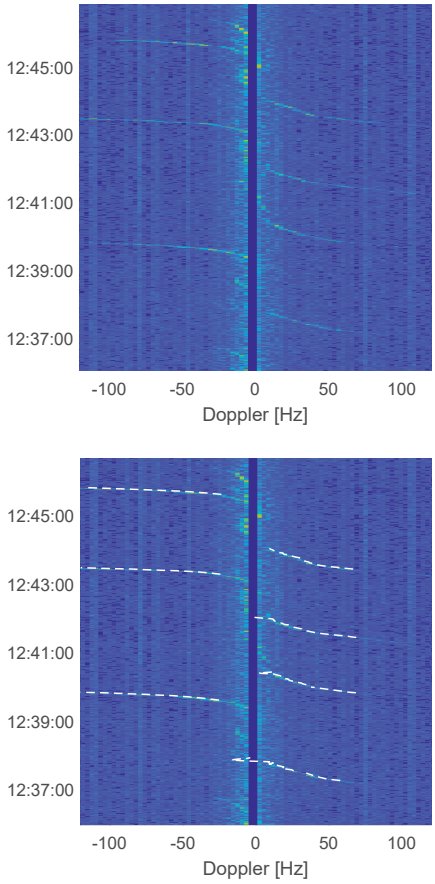

Fig. 4. Doppler vs. time display for transmitter Tx1. The color represents the signal power of the measurement, with yellow indicating high and blue low power values. The contributions of landing (positive Doppler) and starting airplanes(negative Doppler) can be easily identified by increased power values. Additionally, white-colored Range/Doppler (R/D) tracks are shown in the picture below.

B. Localize and classify targets on the runway

a) Localization: The runways are modeled as straight lines, which allows us to describe the target position by the distance relative to a 2D reference point $\boldsymbol{x}_{\text{ref}}$ on the line. For example a corner point of the runway can be chosen as reference point. A point at the runway can than be uniquely defined by

$$(\sin(\theta), \cos(\theta)) \cdot d + \boldsymbol{x}_{\text{ref}},$$

where d represents the distance with respect to the reference point and θ is a fixed angle parameter, describing the orientation of the runway in relation to the reference point. To model the target trajectory and to account for the high maneuverability of the targets during landing or takeoff, we use a 3D evolution model with the state vector $\boldsymbol{d}_k = (d_k, \dot{d}_k, \ddot{d}_k)$, where d_k represents the distance to the reference point at time t_k and $\dot{d}_k$ and $\ddot{d}_k$ represent the velocity and acceleration components, respectively. We use the van Keuk evolution Model [18] (chapter 2) with the transition matrix $\mathbf{F}_{k|k-1}$ given by

$$\mathbf{F}_{k|k-1} = \begin{pmatrix} 1 & \Delta t & 0.5\Delta t^2 \\ 0 & 1 & \Delta t \\ 0 & 0 & e^{-\Delta t/a} \end{pmatrix},$$

where $\Delta t = t_k - t_{k-1}$ represents the time difference, and a is a characteristic value representing the maneuver correlation time.

This model has been selected as it fits well with the provided groundtruth trajectories, as demonstrated in Fig. 5. The approximated velocity component $\dot{d}_k$ reflects the trend

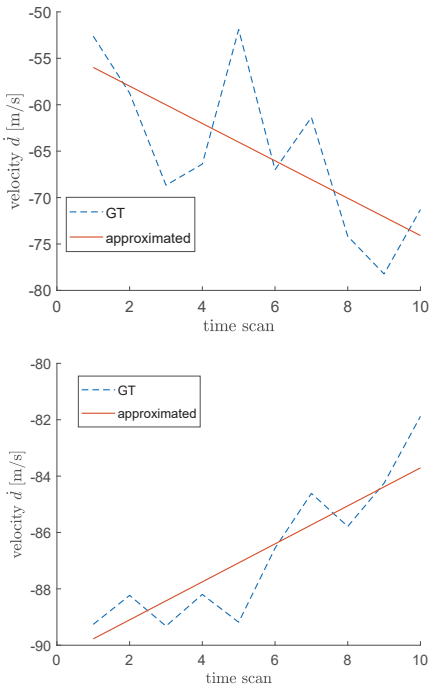

Fig. 5. The van Keuk evolution Model provides a good approximation for modeling trajectories on the runways as shown here exemplary for landing and takeoff.

accurately, even though the GT velocity component is slightly noisy.

To estimate the target trajectory over time based on a set of measurements, from one or multiple R/D tracks from different Tx/Rx pairs, we utilize non-linear regression. In this case, we use the the Matlab function 'nlinfit'. To apply this method, the functional relationship between $\boldsymbol{d}_k$ and a measurement $\mathbf{z}_k^{(i)} = (r_k^{(i)}, \dot{r}_k^{(i)}, \varphi_k^{(i)})$ at time t_k for the ith Tx/Rx pair needs to be described. We define $\boldsymbol{x}_k = \mathbf{g}(\boldsymbol{d}_k)$ to describe the projection from $\boldsymbol{d}_k$ to the Cartesian state (position and velocity) of the target in 2D exploiting the known reference point $\boldsymbol{x}_{\text{ref}}$ and angle θ. Additionally, the measurement function $\mathbf{z}_k^{(i)} = \mathbf{h}^{(i)}(\mathbf{x}_k)$ derived in sec. II is used to model the relationship between the Cartesian state and the measurement parameters. Non-linear regression aims to minimize the sum of squared residuals, which is:

$$\text{ssr} = \sum_{i,k} \frac{({r_k}^{(i)} - h_r^{(i)}(\mathbf{g}(\mathbf{d}_k)))^2}{\sigma_r^2} + \frac{(\dot{r}_k^{(i)} - h_{\dot{r}}^{(i)}(\mathbf{g}(\boldsymbol{d}_k)))^2}{\sigma_{\dot{r}}^2} + \frac{({\varphi_k}^{(i)} - h_\varphi^{(i)}(\mathbf{g}(\boldsymbol{d}_k)))^2}{\sigma_\varphi^2}, \quad (4)$$

where the sum is over all possible time scans and Tx/Rx pairs. Choosing the diagonal matrix $\mathbf{R} = \text{diag}(\sigma_r^2, \sigma_{\dot{r}}^2, \sigma_\varphi^2)$ and the measurement vector $\mathbf{z}_k^{(i)} = (r_k^{(i)}, \dot{r}_k^{(i)}, \varphi_k^{(i)})$, this is equivalent to the sum of Mahalanobis distances:

$$\text{ssr} = \sum_{i,k} (\mathbf{z}_k^{(i)} - \mathbf{h}_k^{(i)}(\mathbf{g}(\boldsymbol{d}_k))^T \mathbf{R}^{-1} (\mathbf{z}_k^{(i)} - \mathbf{h}_k^{(i)}(\mathbf{g}(\boldsymbol{d}_k))). \quad (5)$$

$\mathbf{R}$ serves as a normalizing matrix and is chosen here equal to the measurement noise covariance.

Note that minimizing the Mahalanobis distance is equivalent to maximizing the Likelihood.

b) Classification: The non-linear regression method can provide an estimate even if the target is not located on the runway. The Mahalanobis distance serves as a metric to evaluate the accuracy of the approximated target solution compared to the actual measurements. A decision is made by setting thresholds on this metric, which allows control over the probability of detection and the occurrence of false alarms. Additionally, a maximum distance value can be implemented

V. Evaluation

Different transmitters form different observation regions even when using the same receiver. This is shown in Fig. 6 for two examples of transmitters. The detection region is determined by associating measurements with the GT. If a measurement is associated, the target is declared as detected (see [19] for details). In the example, the first transmitter covers the landing phase and takeoff, while the second transmitter focuses on taxiing.

To evaluate the performance of our detection and tracking approach, we define the following outcomes:

- True Positive (TP): A target is correctly classified as a runway target when an R/D Track is associated with a GT on the runway.
- False Positive (FP): A target is incorrectly classified as a runway target when the corresponding R/D Track cannot be associated with a runway target.
- False Negative (FN): A detected runway target is not identified as such.
- True Negative (TN): A R/D Track is not associated with the GT and not classified as a runway target.

We thus evaluate the classification performance of our approach. The definition of the outcomes is based on the results of the first R/D tracking stage, where a target is declared detected, if it is associated with a GT on the runway.

From this we define the performance metrics:

- true positive rate: $\text{TPR} = \text{TP}/(\text{TP} + \text{FN})$
- true negative rate: $\text{TNR} = \text{TN}/(\text{FP} + \text{TN})$
- positive predictive value: $\text{PPV} = \text{TP}/(\text{TP} + \text{FP})$

for TP outcomes we additionally calculate:

- position error [m]
- ratio of correct runway specification (runway id)
- in case of correct runway specification we also calculate the mean distance error on the runway (distance error [m])

Transmitter Tx1 detects the targets on the runway 1 and 2 (runway numbers are displayed in Fig. 3). So classification also only needs to consider this. The performance measures separated for runways are listed in Tab. I. Additionally, $\text{PPV} = 0.92$ is relatively high, thus only few false tracks are present. Note that position accuracy suffers from poor range accuracy, when using only a single Rx/Tx pair. The

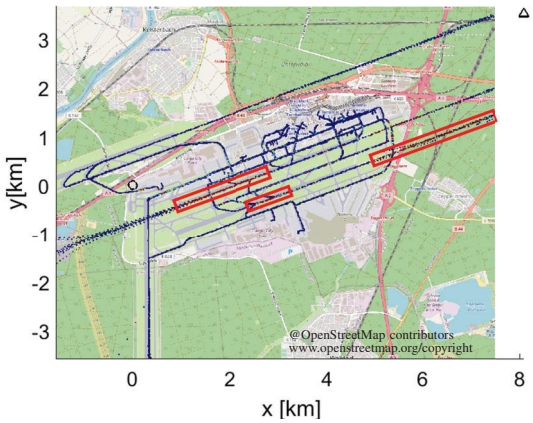

(a) Tx 1

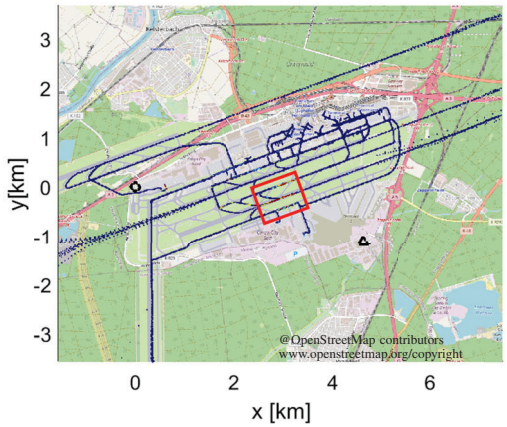

(b) Tx 2

Fig. 6. The detection regions for two different transmitters are displayed by the colorscale of the target trajectories. Red represent a high detection probability. The transmitters are displayed as triangle, the receiver as circle.

TABLE I
PERFORMANCE METRICS FOR TRANSMITTER TX1 SEPARATED FOR DIFFERENT RUNWAYS

runway	TPR	pos. error [m]	runway id	dist. error [m]
1	0.38	1,030.61	0.74	343.03
2	0.75	484.19	0.99	401.32

performance for runway 2 is better than for runway 1 in both the total number of detections and the number of correct runway specification. The increased position error seems to go back to wrong runway specifications, since the distance errors for correct specification are comparable. Following [13] we are interested in finding an optimal threshold for our distance metric, in Tab. II we see that when decreasing the threshold the TPR and the position error decreases, whilst the TNR and PPV values increases. The inital value (first line) seems to be a good choice already. The results have been generated from a one hour recording, including 13 aircrafts landing and 10 aircrafts taking off.

TABLE II
TX1: PERFORMANCE MEASURES FOR DECREASING THE THRESHOLDS FROM TOP TO BOTTOM.

TPR	TNR	PPV	pos. error [m]
0.68	0.84	0.92	688.84
0.67	0.84	0.92	676.7
0.63	0.85	0.92	643.83
0.59	0.85	0.92	596.22
0.55	0.89	0.93	578.26
0.5	0.95	0.97	557.32
0.44	0.97	0.97	455.77
0.35	1	1	423.71
0.21	1	1	420.1
$5.77 \cdot 10^{-2}$	1	1	373.29

TABLE III
PERFORMANCE METRICS FOR TRANSMITTER TX1 SEPARATED FOR DIFFERENT RUNWAYS

runway	TPR	pos. error [m]	runway id	dist. error [m]
1	0.14	718.99	0.2	297.36
1B	0.55	521.86	0.72	399.61
2	0.5	493.1	0.13	86.74
2B	0.4	750.29	0.91	737.94

While Tx1 primarily detects airplanes during takeoff and landing, Tx2 in Fig. 6 (below) is a transmitter that contributes to the taxiing phase. In this case, it also generates detections from the runways in between. For the estimation process, we need to consider four possible runways instead of just two for Tx1. Furthermore, the detection region is relatively small, resulting in a smaller estimation time interval. Note that we use batch processing, where measurements are collected over time before performing non-linear regression. The results were generated with a minimum time interval of 10 seconds, which adds to the time delay of track extraction in R/D tracking. This is a current limitation of implementation, then of course the R/D track history could be used for estimation to reduce the time delay, but has not been implemented yet. As a consequence of the smaller detection regions the TPR value is reduced in comparison to Tx1, see Tab. IV. Also the identification of the specific runway is worse, which might be due to increased ambiguity by considering four instead of two runways. The number of false positives is also increased, see Tab. IV. It is conspicuous that these false tracks correlate in time with the take-offs on runway 1, see Fig. 7(a). We found correlated R/D tracks also in the Doppler vs. time display (Fig. 7(b)). Here, we observe a noticeable deviation from the GT, which is likely attributed to the presence of another GSM transmitter operating on the same frequency as the one being considered. This does not happen regularly for GSM, but goes back to the dense arrangement of transmitters. The handling of correlated events highlights a weakness of the approach when relying solely on a single transmitter for decision making.

For the northern runway the detection regions of two transmitters are shown in Fig. 8. One can observe a significant overlap in the lower section of the runway where airplanes

TABLE IV
TX2: PERFORMANCE MEASURES FOR DECREASING THE THRESHOLD FROM TOP TO BOTTOM.

TPR	TNR	PPV	pos. error [m]
0.54	0.76	0.74	533.32
0.53	0.76	0.74	533.87
0.48	0.78	0.74	521.14
0.41	0.81	0.73	509.64
0.33	0.84	0.72	496.59
0.27	0.88	0.74	503.74
0.2	0.91	0.74	503.81
0.14	0.96	0.82	444.66
$9.7 \cdot 10^{-2}$	0.98	0.88	415.06
$4.16 \cdot 10^{-2}$	1	1	467.63

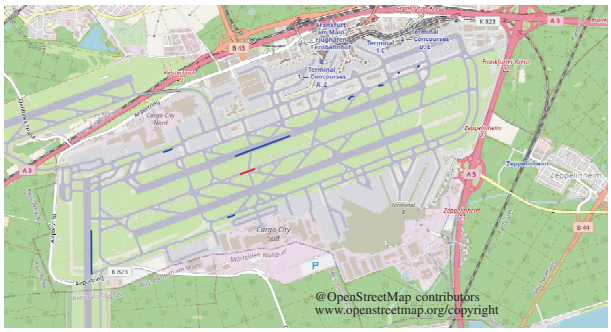

(a) Cartesian display

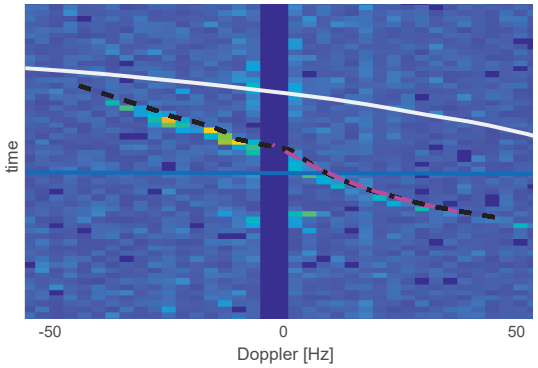

(b) Dopper vs. time display

Fig. 7. (a) A false track is shown in red, and the ground truth is shown in blue. (b) The ground truth is represented in white and the R/D track corresponding to the false track in (a) in black. The magenta line represents the Cartesian track calculated over a time window (converted back to Doppler coordinates).

roll back to the main airport. This allows for combining two transmitters with the single receiver, i.e. using two bistatic pairs for estimation, to overcome the poor position accuracy of a single bistatic pair. In Table V the performance measures are shown. We note a good performance at runway 3B with improved estimation accuracy compared to the single sensor case. However, the detection probability (TPR) decreases as two transmitters are required. Only few false alarms are generated, which is reflected in the values TNR = 0.98 and PPV = 0.85. The high TNR value can be further traced back to a large number of R/D tracks that are not originating from airplanes but are likely coming from car traffic on a nearby

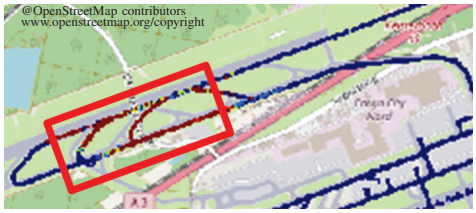

(a) Tx3

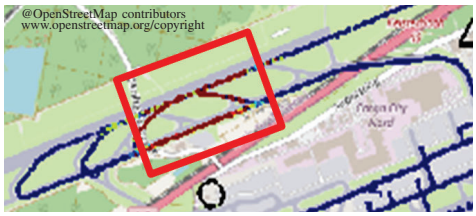

(b) Tx4

Fig. 8. The detection regions for two different transmitters at the northern runway are displayed by the colorscale of the target trajectories. Red represent a high detection probability.

TABLE V
PERFORMANCE METRICS FOR TRANSMITTER TX3 AND TX4 SEPARATED FOR DIFFERENT RUNWAYS

runway	TPR	pos. error [m]	runway id	dist. error [m]
3	0.26	736.95	0	NaN
3B	0.47	189.36	0.97	93.4

highway. The results have been generated from a 45-minute recording, including 11 landing aircrafts.

VI. CONCLUSION

In this paper, we have presented a two-stage strategy for detecting and tracking airplanes on the runway. This strategy involves a detection step and a localization and classification step. The approach was applied to GSM passive radar data obtained during a measurement campaign at Frankfurt Airport in Germany.

We found that different transmitter/receiver (Tx/Rx) pairs cover different regions of the airport. Thus, despite limited range of a single bistatic Tx/Rx pair, the range of the passive radar system can be significantly expanded by increasing the number of used transmitters.

Due to constraining the dimension of the estimation state vector, we demonstrated that track estimation can be performed with only a few contributing Tx/Rx pairs. The estimation approach can be applied for single Tx/Rx pairs or combinations of pairs, if there is an overlap in the detection region. By relying on multiple Tx/Rx pairs for estimation, we showed that we can improve the estimation accuracy and reduce the number of false positives.

Furthermore, our findings indicate that Range/Doppler tracks (which are the result of the first detection stage) exhibit distinct characteristics that can be used to differentiate between different flight paths. Currently, the classification step employs a simple threshold detector, which in future could

be replaced by a more advanced neural network method for enhanced classification and localization. Finally, improving the quality of Range/Doppler tracking by use of track-before-detect algorithms [20], is an ongoing area of research that has the potential to enhance overall performance.

ACKNOWLEDGMENT

This work was funded by the German Ministry of Economic Affairs and Climate Action within the Luftfahrtforschungsprogramm LuFo VI-1 (project Passiv II). We gratefully acknowledge the cooperation with Hensoldt Sensors GmbH, DFS Deutsche Flugsicherung GmbH, Fraport AG and Fraunhofer FHR. In particular, we thank DFS and Fraport AG for the opportunity to conduct the measurements, and we appreciate the diverse support and the provision of the ground truth.

This paper was reviewed and revised in parts with the assistance with an AI-powered tool (based on GPT3.5 by OpenAI) for textual editing and grammatical support.

REFERENCES

[1] Eurocontrol, "Wide area multilateration report on EATMP TRS 131/04 version 1.1," 2005, accessed on march 1, 2024. [Online]. Available: https://www.eurocontrol.int/sites/default/files/2019-05/surveilllance-report-wide-area-multilateration-200508.pdf

[2] Z. Koppanyi and C. K. Toth, "Object tracking with lidar: Monitoring taxiing and landing aircraft," *Applied Sciences*, vol. 8, no. 2, 2018. [Online]. Available: https://www.mdpi.com/2076-3417/8/2/234

[3] Y. Cai, J. Ma, W. Yan, W. Zhang, and Y. An, "Aircraft detection using phase-sensitive optical-fiber OTDR," *Sensors*, vol. 21, no. 15, 2021. [Online]. Available: https://www.mdpi.com/1424-8220/21/15/5094

[4] Rhode&Schwarz, "R&S DF-ATC-S ATC DF System Solution Accurate and reliable direction finding for civil and military air traffic control," accessed on march 6, 2024. [Online]. Available: https://scdn.rohde-schwarz.com/ur/pws/dl_downloads/d\unhbox\voidb@x\bgroup\@xxxiil\egroup_common_library/dl_brochures_and_datasheets/pdf_1/DF-ATC-S_bro_en_5215-0792-12_v0100.pdf

[5] N. J. Willis, *Bistatic Radar*. SciTech Publishing, 2007.

[6] H. Kuschel, J. Heckenbach, S. Mueller, and R. Appel, "On the potentials of passive, multistatic, low frequency radars to counter stealth and detect low flying targets," in *in IEEE Radar Conf.*, may 2008, pp. 1443–1448.

[7] P. Howland, D. Maksimiuk, and G. Reitsma, "FM radio based bistatic radar," *IEE Proceedings - Radar, Sonar and Navigation*, vol. 152, no. 3, pp. 107–115, Jun. 2005.

[8] V. Winkler, D. Fraenken, C. Erhart, O. Zeeb, and S. Lutz, "Multistatic multiband passive radar - architecture and sensor cluster results," in *2019 IEEE Radar Conference (RadarConf)*, 2019, pp. 1–6.

[9] D. Tan, H. Sun, Y. Lu, and W. Liu, "Feasibility analysis of GSM signal for passive radar," in *Proceedings of the 2003 IEEE Radar Conference (Cat. No. 03CH37474)*, 2003, pp. 425–430.

[10] C. Steffes, B. Demissie, B. Knoedler, M. Broetje, M. Mandt, and W. Koch, "Passive radar using mobile communication: A discussion of use cases and feasibility," in *2022 IEEE Radar Conference (RadarConf22)*, 2022, pp. 1–6.

[11] M. Daun, U. Nickel, and W. Koch, "Tracking in multistatic passive radar systems using DAB/DVB-T illumination," *Signal Processing*, 2011.

[12] M. Broetje and W. Koch, "Multistatic tracking for passive radar applications," in *Novel Radar Techniques and Applications*, R. Klemm, U. Nickel, C. Gierull, P. Lombardo, H. Griffiths, and W. Koch, Eds. IET, 2017, pp. 335–372.

[13] M. Huai, C. Miao, Y. Li, Q. Suo, L. Su, and A. Zhang, "Metric learning from probabilistic labels," in *Proceedings of the 24th ACM SIGKDD International Conference on Knowledge Discovery & Data Mining*, Y. Guo and F. Farooq, Eds. New York, NY, USA: ACM, 2018, pp. 1541–1550.

[14] H. Griffiths and C. Baker, "Passive coherent location radar systems. part 1: performance prediction," *Radar, Sonar and Navigation, IEE Proceedings* -, vol. 152, no. 3, pp. 153–159, June 2005.

[15] C. Baker, H. Griffiths, and I. Papoutsis, "Passive coherent location radar systems. part 2: waveform properties," *Radar, Sonar and Navigation, IEE Proceedings* -, vol. 152, no. 3, pp. 160–168, June 2005.

[16] U. Nickel, "System considerations for passive radar with gsm illuminators," in *Phased Array Systems and Technology (ARRAY), 2010 IEEE International Symposium on*, Oct 2010, pp. 189–195.

[17] S. T. Handke, M. Broetje, C. Steffes, and W. Koch, "Mission planning for mobile communication passive radar via an evolutionary algorithm," in *2022 23rd International Radar Symposium (IRS)*, 2022, pp. 338–343.

[18] W. Koch, *Tracking and Sensor Data Fusion*. Berlin, Heidelberg: Springer Berlin Heidelberg, 2014.

[19] M. Broetje, B. Knoedler, and W. Koch, "Evaluation of GSM passive radar data and its use in multistatic tracking," in *2016 19th International Conference on Information Fusion (FUSION)*, 2016, pp. 2275–2282.

[20] B. Knoedler, M. Broetje, C. Steffes, and W. Koch, "Detecting and tracking multiple small UAV using passive radar," in *2023 IEEE Radar Conference (RadarConf23)*, 2023, pp. 1–6.